Oligodiacetylenes

DOI: 10.1002/anie.201307904

Optically Pure, Monodisperse *cis*-Oligodiacetylenes: Aggregation-Induced Chirality Enhancement**

*Erin T. Chernick, Gabor Börzsönyi, Christian Steiner, Maximilian Ammon, David Gessner, Sabine Frühbeißer, Franziska Gröhn, Sabine Maier, and Rik R. Tykwinski**

Abstract: *Conformational changes in the conjugated backbone of poly- and oligodiacetylenes (PDAs and ODAs) play an important role in determining the electronic properties of these compounds. At the same time, conformational changes can also result in a folded structure that shows helical chirality. Using* D*-camphor as a chiral building block, we have designed a high-yielding, iterative synthesis of monodisperse, optically pure cis-oligodiacetylenes (ODAs). cis-ODAs up to the tridecamer have been formed, which is the longest monodisperse cis-ODA reported to date. UV/Vis spectroscopy suggests a large effective conjugation length in THF, likely the result of a linear, planar conformation in this solvent. High-resolution STM/AFM measurements of the nonamer cast from THF onto HOPG show a linear structure. In iPrOH, circular dichroism (CD) spectra suggest the formation of chiral aggregates for ODAs with at least nine* D*-camphor units, based on a strong CD response.*

Polydiacetylenes (PDAs) have been extensively studied,[1] while oligodiacetylenes (ODAs) often serve as useful models to examine or predict the properties of PDAs.[2] For example, it is well known that *trans*-PDAs show chromatic properties, a feature that can be applied to form molecular switches and sensors.[1] The electronic properties of PDAs often depend on their effective conjugation length (ECL)[3] and therefore conformational perturbations are important,[4] such as helical folding of the π-conjugated backbone. *trans*-PDAs/ODAs typically show a higher ECL than *cis*-ODAs, due to the folded conformation of *cis*-ODAs in solution.[5] While a helical conformation may limit the ECL, it confers "handedness", in other words, chirality. The ability to control the "twist-sense" bias of a helical foldamer allows one to manipulate chirality, opening doors to applications as chiral molecular sensors and switches[6] and as chiral conducting polymers.[7]

trans-PDAs/ODAs are well known since the pioneering work of Wegner,[8] while much less is known about *cis*-PDAs/ODAs.[9] To date, *cis*-ODAs have only been formed by iterative synthetic routes.[5,10] An efficient *cis*-ODA synthesis must prevent *cis–trans* isomerization, which can be achieved through use of a ring system to enforce the *cis* geometry. Examples of this strategy include the use of a cyclopentene ring reported by Hirsch and co-workers,[5] and using an aryl ring to give the structurally related class of oligomers, the *ortho*-arylenethynylenes.[11]

We envisioned a chiral hydrocarbon ring for the development of optically pure, monodisperse ODAs, whose conformation might be dynamically controlled by solvophobic interactions.[12,13] Several design criteria were crucial to achieve this goal; namely the building block must: 1) prevent *cis–trans* isomerization of the olefin, 2) offer a source of chirality and solubility, and 3) not conjugate into the backbone so that studies reflect only the properties of the enyne framework. Finally, the group should be hydrophobic, enabling solvent-driven assembly to form chiral secondary structures. D-Camphor was identified as a suitable building block, and we report herein the synthesis and characterization of optically pure, monodisperse *cis*-ODAs with unique and switchable chirooptical properties (Figure 1).

Readily available (+)-3-bromocamphor provided the synthetic basis for the desired ODAs (Scheme 1), and it was converted to the bromovinyl triflate **1** by an adaptation of a published protocol.[14] Initial attempts to use **1** in a Sonogashira cross-coupling reaction[15] with trimethylsilylacetylene (TMSA) were surprisingly unsuccessful. Negishi coupling,[16] on the other hand, resulted in selective functionalization at the vinyl triflate and furnished **2** in 82% yield. Attempted

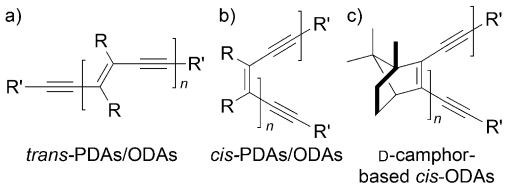

Figure 1. Generic structures of a) *trans*-polydiacetylenes (*trans*-PDAs) and *trans*-oligodiacetylenes (*trans*-ODAs), b) *cis*-PDAs and *cis*-ODAs, and c) D-camphor-based *cis*-ODAs.

[*] Dr. E. T. Chernick, Dr. G. Börzsönyi, Prof. Dr. R. R. Tykwinski
Department of Chemistry and Pharmacy
and Interdisciplinary Center of Molecular Materials (ICMM)
University of Erlangen-Nuremburg
Henkestrasse 42, 91054 Erlangen (Germany)
E-mail: rik.tykwinski@fau.de
Homepage: http://www.chemie.uni-erlangen.de/tykwinski
M. Ammon, D. Gessner, Prof. Dr. S. Maier
Department of Physics, University of Erlangen-Nürnberg
Erwin-Rommel-Strasse 1, 91058 Erlangen (Germany)
S. Frühbeißer, Prof. Dr. F. Gröhn
Department of Chemistry and Pharmacy
and Interdisciplinary Center of Molecular Materials (ICMM)
Egerlandstrasse 3, 91058 Erlangen (Germany)

[**] Funding from the University of Erlangen-Nuremberg, the Cluster of Excellence "Engineering of Advanced Materials" at the University of Erlangen-Nuremberg, the Deutsche Forschungsgemeinschaft (DFG; SFB 953: "Synthetic Carbon Allotropes"), the Interdisciplinary Center for Molecular Materials (ICMM), and the Bavarian Academy of Science is gratefully acknowledged.

Supporting information for this article is available on the WWW under http://dx.doi.org/10.1002/anie.201307904.

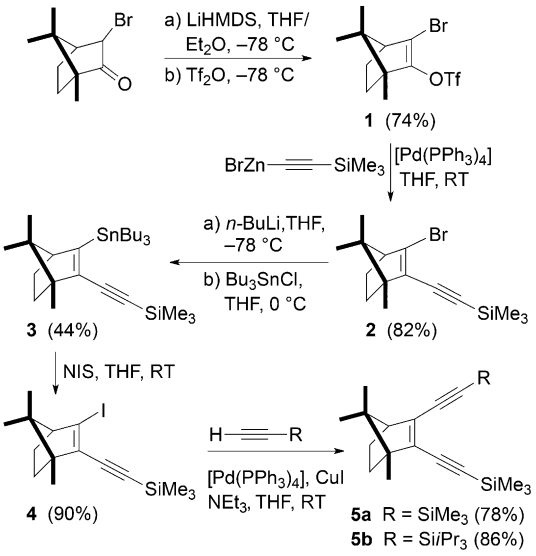

Scheme 1. Synthetic route to ODA monomers **5a**,**b**. LiHMDS = lithium hexamethyldisilazide, NIS = *N*-iodosuccinimide.

cross-coupling of **2** with either TMSA or triisopropylsilylacetylene (TIPSA) under either Sonogashira or Negishi conditions offered only traces of the desired enediyne product. Thus, vinyl bromide **2** was converted to vinyl stannane **3** and then vinyl iodide **4** using a protocol developed by Knochel et al.[17] Vinyl iodide **4** readily reacted with TMSA or TIPSA under Pd catalysis to provide **5a** (78%) and **5b** (86%) in good yield.

The initial chain-elongation protocol appended two camphor units to the nascent oligomer backbone per coupling step (Scheme 2). Exhaustive desilylation of **5a** gave the terminal acetylene, which efficiently reacted with vinyl iodide **4** under Sonogashira coupling conditions to give trimer **6**. Repetition of this desilylation and Pd-catalyzed cross-coupling sequence produced pentamer **7** (73%), heptamer **8** (87%), nonamer **9** (64%), undecamer **10** (77%), and tridecamer **11** (71%) in satisfactory yields. Compounds **6**–**11** form Series A of the optically pure *cis*-ODAs, and to our knowledge, compounds **8**–**11** are the longest monodisperse *cis*-ODAs reported to date.[18]

The synthetic protocol for ODA Series A gives oligomers composed only of an odd number of repeat units. Oligomers in Series A also possess a regiochemical "disconnect" at the central camphor unit arising from the initial deprotection and coupling sequence with **5a**. It was not known whether either, or both, of these factors might influence conjugation through the ODA framework. Therefore, Series B ODAs were assembled in which the chain length was increased by only a single camphor unit per desilylation/cross-coupling iteration (Scheme 3). Briefly, the trimethylsilyl group of compound **5b** was removed and this product used in a cross-coupling reaction with vinyl iodide **4** to give dimer **12**. Elongation of the oligomer was subsequently accomplished to give trimer **13**

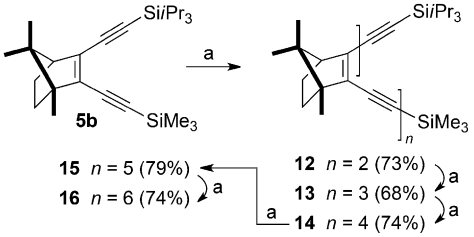

Scheme 3. Synthesis of ODAs **12**–**16** (Series B). Reagents and conditions: a) 1. K_2CO_3, MeOH/THF, RT; 2. **4**, $[Pd(PPh_3)_4]$, CuI, NEt_3, THF, RT.

(68%), tetramer **14** (74%), pentamer **15** (79%), and hexamer **16** (74%). By the length of the hexamer **16**, it was clear that the electronic absorption behavior of Series A and B are quite similar, and the rather laborious chain extension of Series B was abandoned.

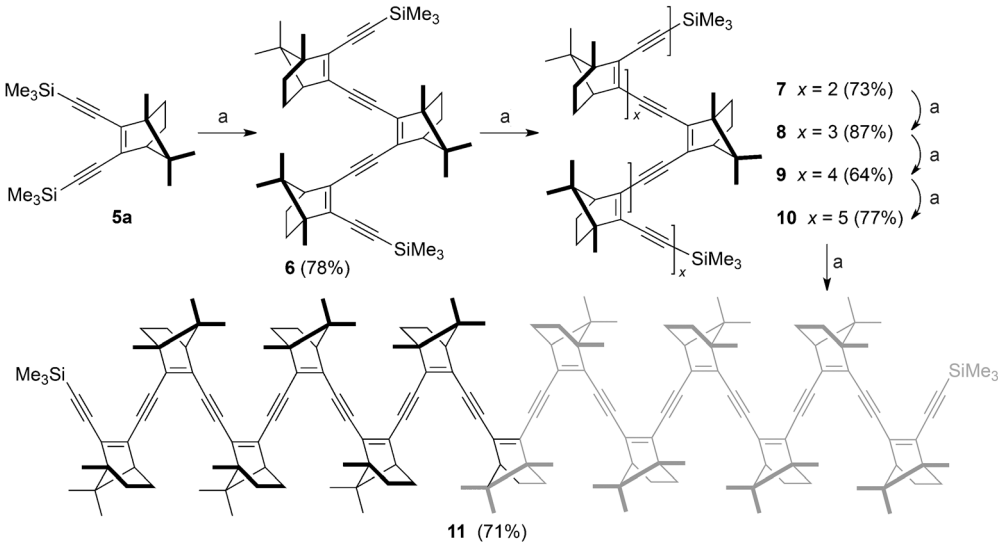

Scheme 2. Synthesis of ODAs **6**–**11** (Series A). Reagents and conditions: a) 1. K_2CO_3, MeOH/THF, RT; 2. **4**, $[Pd(PPh_3)_4]$, CuI, NEt_3, THF, RT. For tridecamer **11**, the gray and black colors designate "halves" of the molecule created by the regiochemical disconnect at the center camphor unit (see text for discussion).

We measured the UV/Vis spectra of the ODAs in THF solution (ca. > 1 mM). The electronic absorption characteristics versus length for the ODAs are obvious, from the colorless dimer (**12**) through the orange tri- and tetramers (**6**, **13**, **14**), to the red pentamers (**7** and **15**) and beyond. The UV/Vis absorptions of Series A ODAs (THF) are shown in Figure 2 (Series B are found in Figure S1), and λ_{max} values are listed in Table 1. Absorption trends versus length for Series A and B are similar, suggest-

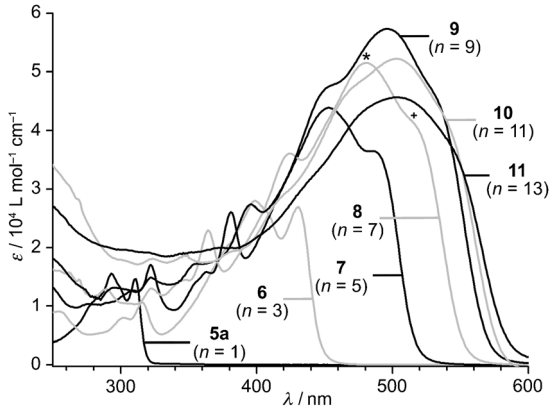

Figure 2. UV/Vis spectra of ODA Series A as measured in THF, *n* is the number of enyne units (λ_{max1} and λ_{max2} are identified with * and +, respectively, for heptamer **8**; see text for discussion).

Table 1: Electronic absorption properties of the ODAs **6**–**16** measured in THF.

Compound	*n*[a]	λ_{max1} [nm] ([eV])	λ_{max2} [nm] ([eV])
12	2	357 (3.5)	382 (3.2)
6	3	399 (3.1)	430 (2.9)
13	3	400 (3.1)	430 (2.9)
14	4	432 (2.9)	465 (2.7)
7	5	453 (2.7)	492 (2.5)
15	5	454 (2.7)	492 (2.5)
16	6	471 (2.6)	510 (2.4)
8	7	480 (2.6)	524 (2.4)[b]
9	9	496 (2.5)	538 (2.3)[b]
10	11	502 (2.5)	545 (2.3)[b]
11	13	504 (2.5)	553 (2.2)[b]

[a] *n* is the number of D-camphor enyne units in the ODA. [b] Estimated from shoulder absorption by deconvolution of the spectra.

ing a minimal electronic influence from the regiochemical disconnect in Series A.[19] For shorter oligomers ($n \leq 6$), two distinct λ_{max} values are found: λ_{max1} at higher energy and λ_{max2} at lower energy (labeled * and +, respectively, for heptamer **8** in Figure 2). Values for λ_{max1} and λ_{max2} show a consistent decrease in the energy as a function of increasing oligomer length, reaching a value of $\lambda_{max2} = 553$ nm (2.2 eV) for the tridecamer **11**.[20] It is evident from the spectra in Figure 2 that λ_{max} values are reaching the ECL, that is, the length at which additional repeat units (*n*) no longer reduce the energy of λ_{max}. Meier and co-workers have suggested an empirical method to estimate the saturation value for optical absorptions in conjugated polymers and to provide an estimate of ECL.[3a] The λ_{max2} values of **6**–**16** have been analyzed following the Meier protocol which gives an estimate of $\lambda_\infty = (556 \pm 1.0)$ nm (2.2 eV) at an ECL of $n_{ECL} = 17$ (see Figure S2). This is a surprising result, since λ_∞ is at much lower energy than suggested by, for example, Takayama and co-workers, who predicted λ_∞ for *cis*-ODAs to be roughly 345 nm with an $n_{ECL} \leq 5$ (presumably due to folded structures in solution).[10] On the other hand, literature reports for *trans*-ODAs offer estimates from $\lambda_\infty = 494$ nm ($n_{ECL} \approx 8$),[2d] $\lambda_\infty = 532$ nm (n_{ECL} not provided),[21] to $\lambda_\infty = 551$ nm ($n_{ECL} = 10$).[22]

Brédas and co-workers have examined the origin of n_{ECL} values in terms of the energy barrier to rotation about a C_{sp}–C_{sp2} bond (torsional barrier) in *trans*-ODAs.[4] This work suggests $n_{ECL} \approx 6$ for *trans*-ODAs, which corresponds to a torsional barrier of roughly 1.8 kcal mol^{-1}. By comparison, the value of $n_{ECL} = 17$ for **6**–**16** suggests that these ODAs maintain a planar, conjugated conformation in THF with a relative high C_{sp}–C_{sp2} rotational barrier of approximately 4.7 kcal mol^{-1}.[4] Three factors, in principle, govern deviations from a planar structure in **6**–**16**, 1) the the barrier to rotation about the C_{sp}–C_{sp2} bond, 2) the strength of interactions between the pendent camphor groups and solvent in a planar structure, and 3) favorable intramolecular interactions between camphor units in a folded, nonplanar structure. Thus, moving from THF to a more hydrophilic solvent should favor a nonplanar and, perhaps, folded helical conformation. Following this hypothesis, UV/Vis absorption profiles for ODAs were examined in *i*PrOH. ODAs with $n \geq 9$ show a significant blue shift for λ_{max} values relative to those measured in THF; for example, nonamer **9** shows $\lambda_{max} =$ 438 nm in *i*PrOH (Figure S3). This switch in the absorption profile is also concentration dependent; for **9** it occurs at concentrations greater than 0.01 mM in *i*PrOH, which suggests that it originates from intermolecular interactions (i.e., aggregation). Variable-temperature (VT) UV/Vis experiments for **9** were carried out from 20–70 °C (Figure 3a) and show that aggregation is reversible. As the temperature is increased, λ_{max} undergoes a red shift, and the spectral features at 70 °C are analogous those found for **9** in THF; in other words, the molecule is switched to an extended, planar conformation.

Circular dichroism (CD) spectra of ODAs measured in THF show no significant Cotton effect (e.g., nonamer **9** in Figure 3b), consistent with an extended planar structure. Conversely, a strong Cotton effect is observed in spectra ODAs **9**–**11** measured in *i*PrOH, indicating a chiral conformation during aggregation,[23] as demonstrated for nonamer **9** in Figure 3b.[24] The CD spectra of **9** in *i*PrOH are temperature dependent. The intensity of the CD signal steadily decreases upon heating and disappears completely by 70 °C (Figure 3a). The change in the CD signal is concurrent with a shift in the UV/Vis spectra from an "aggregated" profile at 20 °C to that of an extended, planar ODA at 70 °C. When the sample is cooled, the original CD and UV/Vis profiles are restored, indicating that the chiral aggregates are re-established. Thus, the aggregation is fully reversible.[25]

Dynamic light-scattering (DLS) experiments were performed on solutions of **9** to shed light on the aggregates and aggregation process in *i*PrOH (Figures S4 and S5). As expected, based on the UV/Vis and CD experiments, no aggregates were observed for DLS analyses of **9** in THF. In *i*PrOH (1 μM and 2 μM solutions), however, measurements of **9** showed a variety of particle sizes with hydrodynamic radii ranging from $R_H = 8$ nm to $R_H = 370$ nm. Time-dependent light-scattering measurements reveal no distinct trend in aggregation versus time other than that aggregation is spontaneous in *i*PrOH and larger aggregates are formed at higher concentrations.

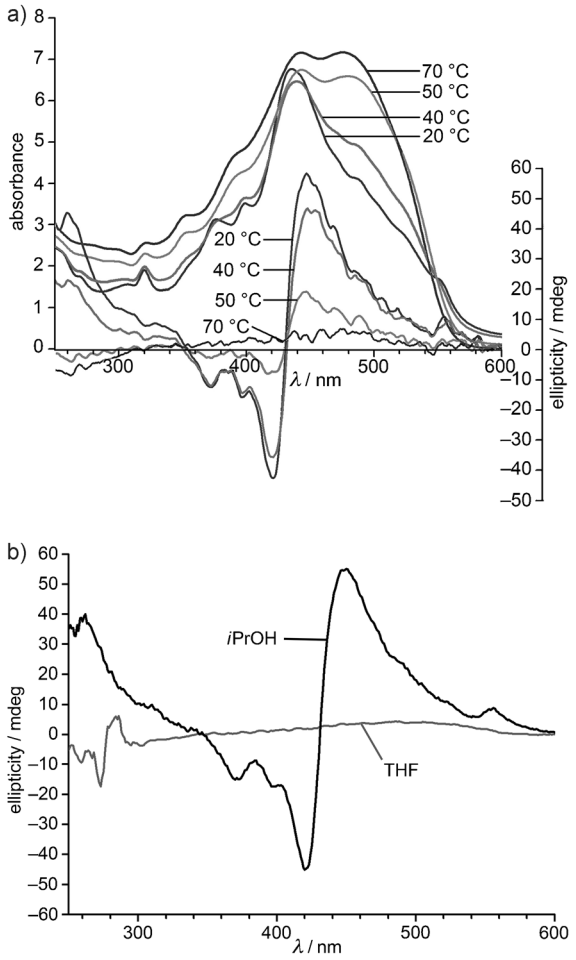

Figure 3. a) VT UV/Vis and CD spectra of nonamer **9** in *i*PrOH and b) CD spectra of nonamer **9** in *i*PrOH (1.2 μM) and THF (0.82 μM).

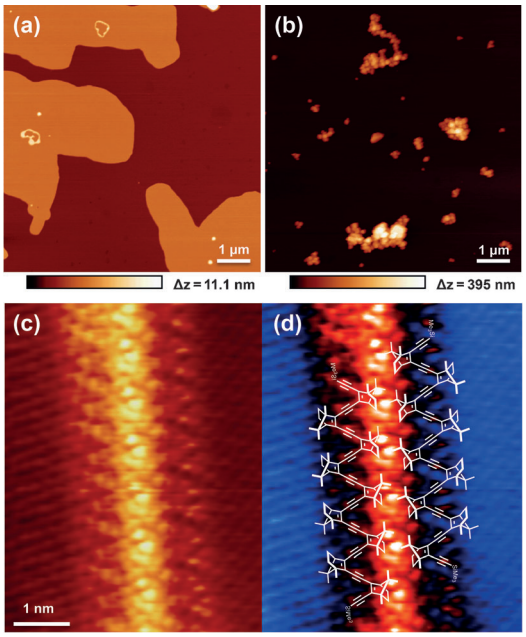

Figure 4. a,b) AFM topographies (recorded in tapping mode) showing the solvent-dependent aggregation of **9** drop-cast on a mica surface from a) THF solution and b) *i*PrOH solution at a concentration of 2 μM. c,d) Low-temperature constant-current STM image of **9** drop-cast on HOPG from THF (0.1 μM) along with a possible molecular arrangement in (d). Note that the HOPG lattice of the substrate is resolved on either side of the molecules ($U = -1.4$ V, $I = 107$ pA).

The aggregation of oligomer **9** was explored by scanning tunneling microscopy (STM) and atomic force microscopy (AFM) measurements. From these studies, it is clear that the behavior of **9** on surfaces is also strongly solvent dependent. Nonamer **9** forms a film when drop-cast from THF (2 μM) onto either mica or HOPG (Figure 4a). On the other hand, drop-casting from *i*PrOH on mica produces clusters that are several hundred nanometers in size (Figure 4b). Molecularly resolved STM measurements of **9** adsorbed on HOPG from THF solution also support a planar geometry for the ODA (Figures 4c,d).[26] An unambiguous model for the assembly or ordering of **9** could not, however, be assigned due to the complex appearance in the STM images. Scanning tunneling spectroscopy shows distinct peaks at −1.8 V and +0.4 V (Figure S6), which are attributed to the HOMO and LUMO, respectively. STM measurements thus predict a HOMO–LUMO gap of 2.2 eV, which closely matches the values obtained by UV/Vis absorption studies.

We have successfully synthesized optically pure *cis*-ODAs with a maximum oligomer length reaching 13 repeat units, which are the longest *cis*-ODAs reported to date. These *cis*-ODAs show a bathochromic shift in the UV/Vis absorption maxima versus oligomer length, and a limiting value of $\lambda_{max} =$ 556 nm at the effective conjugation length of $n_{ECL} = 17$. The unexpectedly low absorption energy for the longest ODAs indicates that the oligomers exist in a planar, extended conformation in THF. UV/Vis and CD spectroscopic measurements in *i*PrOH imply that oligomers $n \geq 9$ undergo solvophobic-induced chiral aggregation. This premise is supported by AFM, STM, and DLS analyses. The chiral aggregation is temperature dependent and reversible. To our knowledge, this is the first example of chiral aggregates based on *cis*-ODAs. The exact conformation and composition of these chiral aggregates have yet to be determined, and further studies are underway to elucidate more defined details.

Received: September 8, 2013
Published online: November 29, 2013

Keywords: chirality · *cis*-oligodiacetylenes · foldamers · monodispersity · thermochromic switches

[1] a) S. Okada, S. Peng, W. Spevak, D. Charych, *Acc. Chem. Res.* **1998**, *31*, 229–239; b) B. Yoon, S. Lee, J.-M. Kim, *Chem. Soc. Rev.* **2009**, *38*, 1958–1968; c) D. J. Ahn, S. Lee, J.-M. Kim, *Adv. Funct. Mater.* **2009**, *19*, 1483–1496; d) X. Chen, G. Zhou, X. Peng, J. Yoon, *Chem. Soc. Rev.* **2012**, *41*, 4610–4630.

[2] a) H. J. Byrne, W. Blau, R. Giesa, R. C. Schulz, *Chem. Phys. Lett.* **1990**, *167*, 484–489; b) C. C. J. Hendrikx, M. Polhuis, A. Pul-Hootsen, R. B. M. Koehorst, A. van Hoek, H. Zuilhof, E. J. R. Sudhölter, *Phys. Chem. Chem. Phys.* **2005**, *7*, 548–553; c) G. S. Pilzak, J. Baggerman, B. van Lagen, M. A. Posthumus, E. J. R. Sudhölter, H. Zuilhof, *Chem. Eur. J.* **2009**, *15*, 2296–2304;

d) G. S. Pilzak, B. van Lagen, C. C. J. Hendrikx, E. J. R. Sudhölter, H. Zuilhof, *Chem. Eur. J.* **2008**, *14*, 7939 – 7950.
[3] a) H. Meier, U. Stalmach, H. Kolshorn, *Acta Polym.* **1997**, *48*, 379 – 384; c) R. E. Martin, F. Diederich, *Angew. Chem.* **1999**, *111*, 1440 – 1469; *Angew. Chem. Int. Ed.* **1999**, *38*, 1350 – 1377; b) J. Rissler, *Chem. Phys. Lett.* **2004**, *395*, 92 – 96.
[4] J. S. Sears, R. R. Chance, J.-L. Brédas, *J. Am. Chem. Soc.* **2010**, *132*, 13313 – 13319.
[5] C. Kosinski, A. Hirsch, F. W. Heinemann, F. Hampel, *Eur. J. Org. Chem.* **2001**, 3879 – 3890.
[6] a) E. Ohta, H. Sato, S. Ando, A. Kosaka, T. Fukushima, D. Hashizume, M. Yamasaki, K. Hasegawa, A. Muraoka, H. Ushiyama, K. Yamashita, T. Aida, *Nat. Chem.* **2011**, *3*, 68 – 73; b) E. Yashima, K. Maeda, H. Iida, Y. Furusho, K. Nagai, *Chem. Rev.* **2009**, *109*, 6102 – 6211.
[7] L. A. P. Kane-Maguire, G. G. Wallace, *Chem. Soc. Rev.* **2010**, *39*, 2545 – 2576.
[8] G. Wegner, *Z. Naturforsch. B* **1969**, *24*, 824 – 832.
[9] G. W. Coates, A. R. Dunn, L. M. Henling, D. A. Dougherty, R. H. Grubbs, *Angew. Chem.* **1997**, *109*, 290 – 293; *Angew. Chem. Int. Ed. Engl.* **1997**, *36*, 248 – 251.
[10] Y. Takayama, C. Delas, K. Muraoka, M. Uemura, F. Sato, *J. Am. Chem. Soc.* **2003**, *125*, 14163 – 14167.
[11] a) T. V. Jones, M. M. Slutsky, R. Laos, T. F. A. de Greef, G. N. Tew, *J. Am. Chem. Soc.* **2005**, *127*, 17235 – 17240; b) J. He, J. L. Crase, S. H. Wadumethrige, K. Thakur, L. Dai, S. Zou, R. Rathore, C. S. Hartley, *J. Am. Chem. Soc.* **2010**, *132*, 13848 – 13857; c) B.-B. Ni, Q. Yan, Y. Ma, D. Zhao, *Coord. Chem. Rev.* **2010**, *254*, 954 – 971; d) W. Lu, W.-M. Kwok, C. Ma, C. T.-L. Chan, M.-X. Zhu, C.-M. Che, *J. Am. Chem. Soc.* **2011**, *133*, 14120 – 14135.
[12] a) D. J. Hill, M. J. Mio, R. B. Prince, T. S. Hughes, J. S. Moore, *Chem. Rev.* **2001**, *101*, 3893 – 4011; b) S. H. Gellman, *Acc. Chem. Res.* **1998**, *31*, 173 – 180.
[13] a) M. A. Gin, T. Yokozawa, R. B. Prince, J. S. Moore, *J. Am. Chem. Soc.* **1999**, *121*, 2643 – 2644; b) C. A. Lewis, R. R. Tykwinski, *Chem. Commun.* **2006**, 3625 – 3627.
[14] I. Ilaldinov, S. Bukharov, R. Kadyrov, *Russ. J. Org. Chem.* **2007**, *43*, 747 – 752.
[15] K. Sonogashira, Y. Tohda, N. Hagihara, *Tetrahedron Lett.* **1975**, *16*, 4467 – 4470; R. R. Tykwinski, *Angew. Chem.* **2003**, *115*, 1604 – 1606; *Angew. Chem. Int. Ed.* **2003**, *42*, 1566 – 1568; R. Chinchilla, C. Najera, *Chem. Rev.* **2007**, *107*, 874 – 922.
[16] E. Negishi, X. Zeng, Z. Tan, M. Qian, Q. Hu in *Metal-Catalyzed Cross-Coupling Reactions*, 2nd ed. (Eds.: A. de Meijere, F. Diederich), Wiley-VCH, Weinheim, **2004**, chap. 15.
[17] C. Despotopoulou, R. C. Bauer, A. Krasovskiy, P. Mayer, J. M. Stryker, P. Knochel, *Chem. Eur. J.* **2008**, *14*, 2499 – 2506.
[18] The longest all-carbon *cis*-ODA that has been synthesized and reported to date is a pentamer (see Ref. [10]), and a hexamer containing heteroatoms in the annulated cycles is also known, see: M. Kim, D. Lee, *J. Am. Chem. Soc.* **2005**, *127*, 18024 – 18025.
[19] The only obvious difference between the UV/Vis spectra of Series A and B is the slightly higher ε values for Series B.
[20] If one considers the onset of absorption to be 585 nm, the band gap for **11** is estimated to be roughly 2.1 eV.
[21] F. Wudl, S. P. Bitler, *J. Am. Chem. Soc.* **1986**, *108*, 4685 – 4687.
[22] R. Giesa, R. C. Schulz, *Polym. Int.* **1994**, *33*, 43 – 60.
[23] Chiral amplification by aggregation is well established, see for examples: a) P. Rivera-Fuentes, J. L. Alonso-Gómez, A. G. Petrovic, F. Santoro, N. Harada, N. Berova, F. Diederich, *Angew. Chem.* **2010**, *122*, 2296 – 2300; *Angew. Chem. Int. Ed.* **2010**, *49*, 2247 – 2250; b) M. M. J. Smulders, I. A. W. Filot, J. M. A. Leenders, P. van der Schoot, A. R. A. Palmans, A. P. H. J. Schenning, E. W. Meijer, *J. Am. Chem. Soc.* **2010**, *132*, 611 – 619; c) A. R. A. Palmans, E. W. Meijer, *Angew. Chem.* **2007**, *119*, 9106 – 9126; *Angew. Chem. Int. Ed.* **2007**, *46*, 8948 – 8968.
[24] The crossover point of the CD couplet corresponds to λ_{max} in the UV/Vis spectrum, suggesting excitonic coupling between enyne chromophores.
[25] Over the course of several hours aggregates of **9** precipitate out of *i*PrOH solution (see Figure S7), which results in the disappearance of the CD signal. The aggregation process is reversible, and when the precipitate is redissolved upon heating or sonication, the CD signal is regenerated.
[26] Subtle differences in the STM contrast recorded at different bias voltages indicate that the ends of single molecules of **9** are in a linear arrangement.

